SUPPLEMENTARY INFORMATION

Title: Measuring cell cycle-dependent DNA damage responses and p53 regulation on a cell-by-cell basis from image analysis

Authors and affiliations: S. Dhuppar[1] and Aprotim Mazumder[1,*]

[1]TIFR Centre for Interdisciplinary Sciences, TIFR Hyderabad, 36/P, Gopanpally, Serlingampally Mandal, Hyderabad - 500107, Telangana, India.

*Correspondence: aprotim@tifrh.res.in

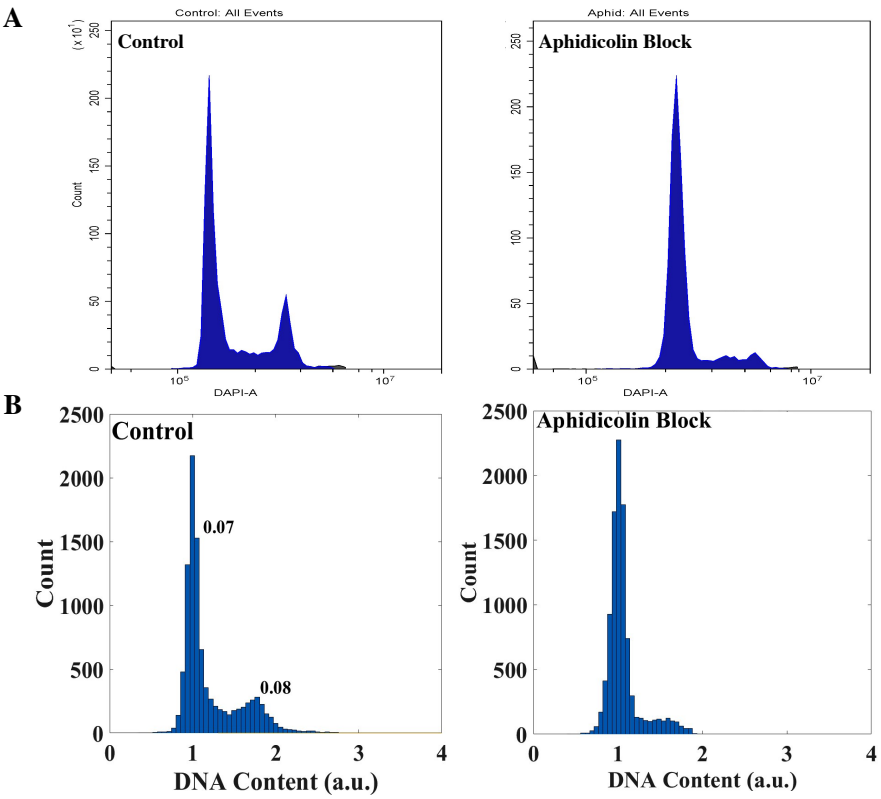

Supplementary Figure S1: Quality of DNA content histogram from imaging is comparable with that from the conventional flow cytometry

(A) DNA content of HeLa cells (mock-treated and synchronized) analyzed with the flow cytometer (9700 cells) (Cytoflex-S). It established the dosage of aphidicolin and the time required to arrest the cells (10 μg/ml for 30 hours). (B) The same data obtained from the cytometer were analyzed using Matlab. The coefficients of variation for G1- and G2-peak obtained for flow cytometry were comparable with that from imaging at 40X.

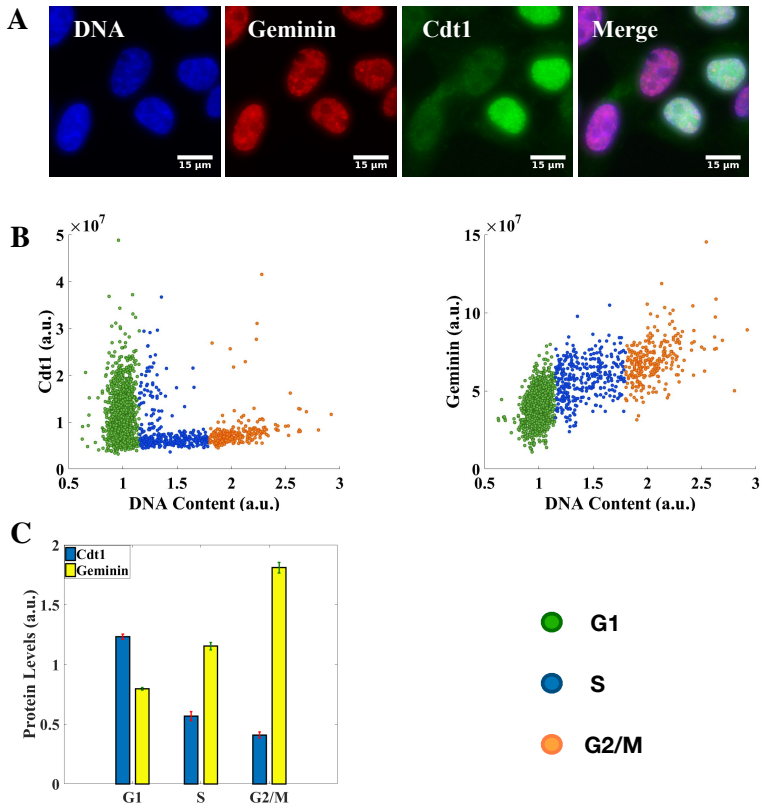

Supplementary Figure S2-A: Cell cycle staging from imaging conforms with the expression profiles of standard cell cycle markers – geminin and cdt1

(A) IF was performed for geminin and cdt1on HeLa cells (scale bar 15 μm). (B) Cell cycle distribution of geminin and cdt1. (C) Mean levels of geminin and cdt1 in respective phases of the cell cycle. The expression profiles for them were opposite. Protein levels, here, were normalized with respect to the respective means of the populations comprising cells from all the phases of the cell cycle. (Error bars are standard errors. The analysis was done on 1700 cells.)

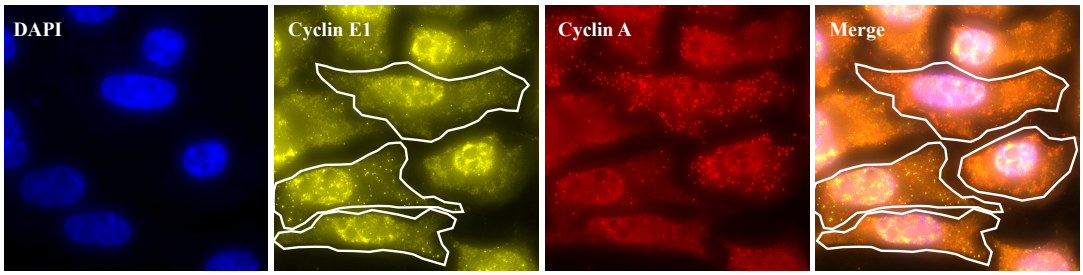

Supplementary Figure S2-B: Manual segmentation with the help of intensities from autofluorescence and non-specific binding

An example of manual segmentation of cells (the same field as shown in Figure 2; mRNA channels here are contrast-adjusted to show cell boundaries). The cells for which the boundaries were ambiguous were discarded from further analysis.

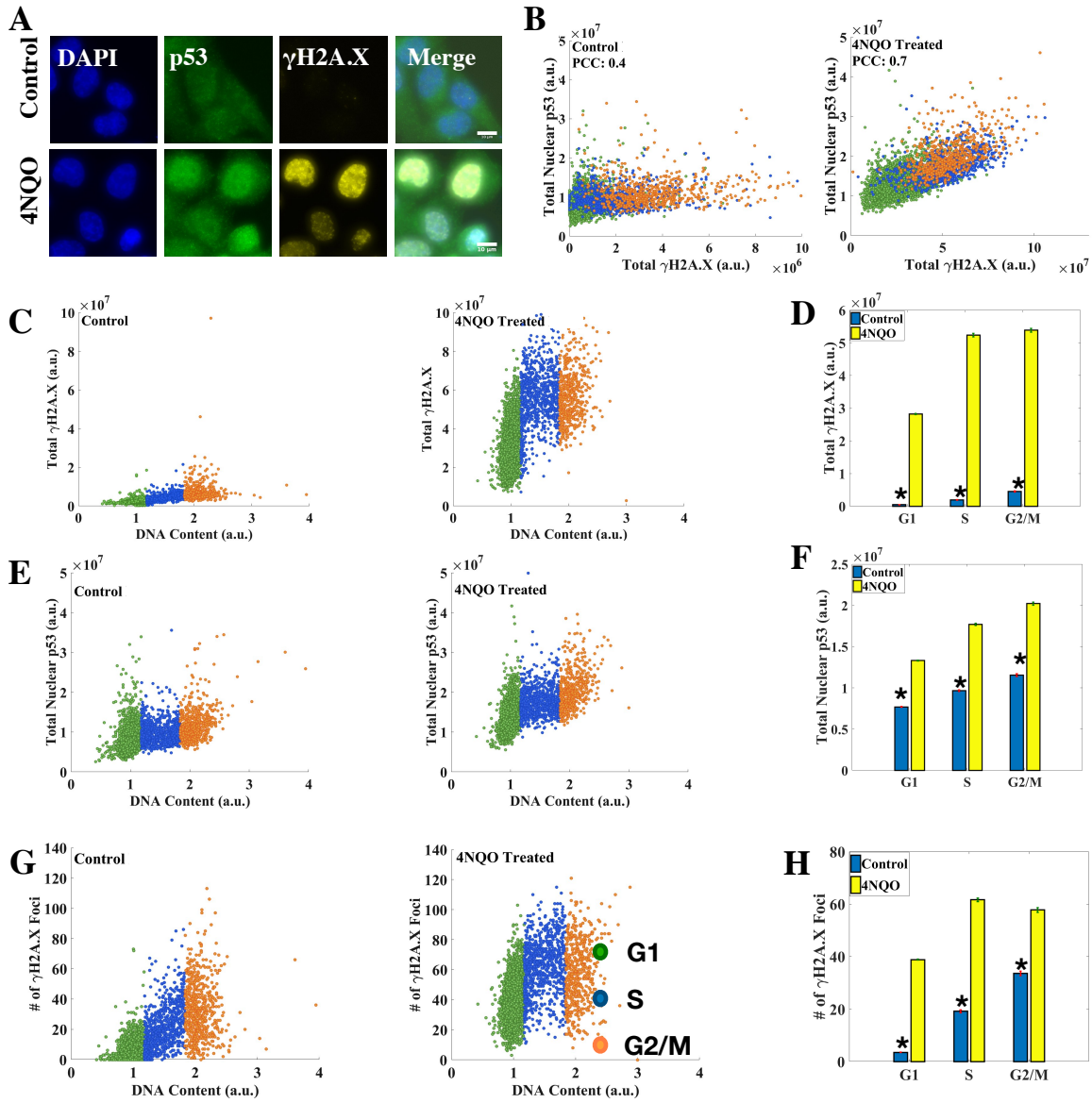

Supplementary Figure S3: Correlation between p53 and γH2A.X increases in DNA damaged cells

(A) IF was done for p53 and γH2A.X on HeLa cells (scale bar: 10 μm). (B) Correlation between γH2A.Xand p53 levels increased in DNA damaged cells. (C, E) Cell cycle distribution of γH2A.X and p53 in DNA damaged and control cells. γH2A.X levels linearly increased in control cells while they peaked in the S-phase in DNA damaged cells. (D) Large induction of γH2A.X in DNA damaged cells in all the phases of the cell cycle. (F) Significant induction of p53 in DNA damaged cells. (G) Foci counting algorithm in Matlab. (H) γH2A.X foci distribution in control and DNA damaged cells. All differences are significant with p-value < 0.05 (K-S test). (Errorbars are standard errors. The analysis was done on 5000 cells.)

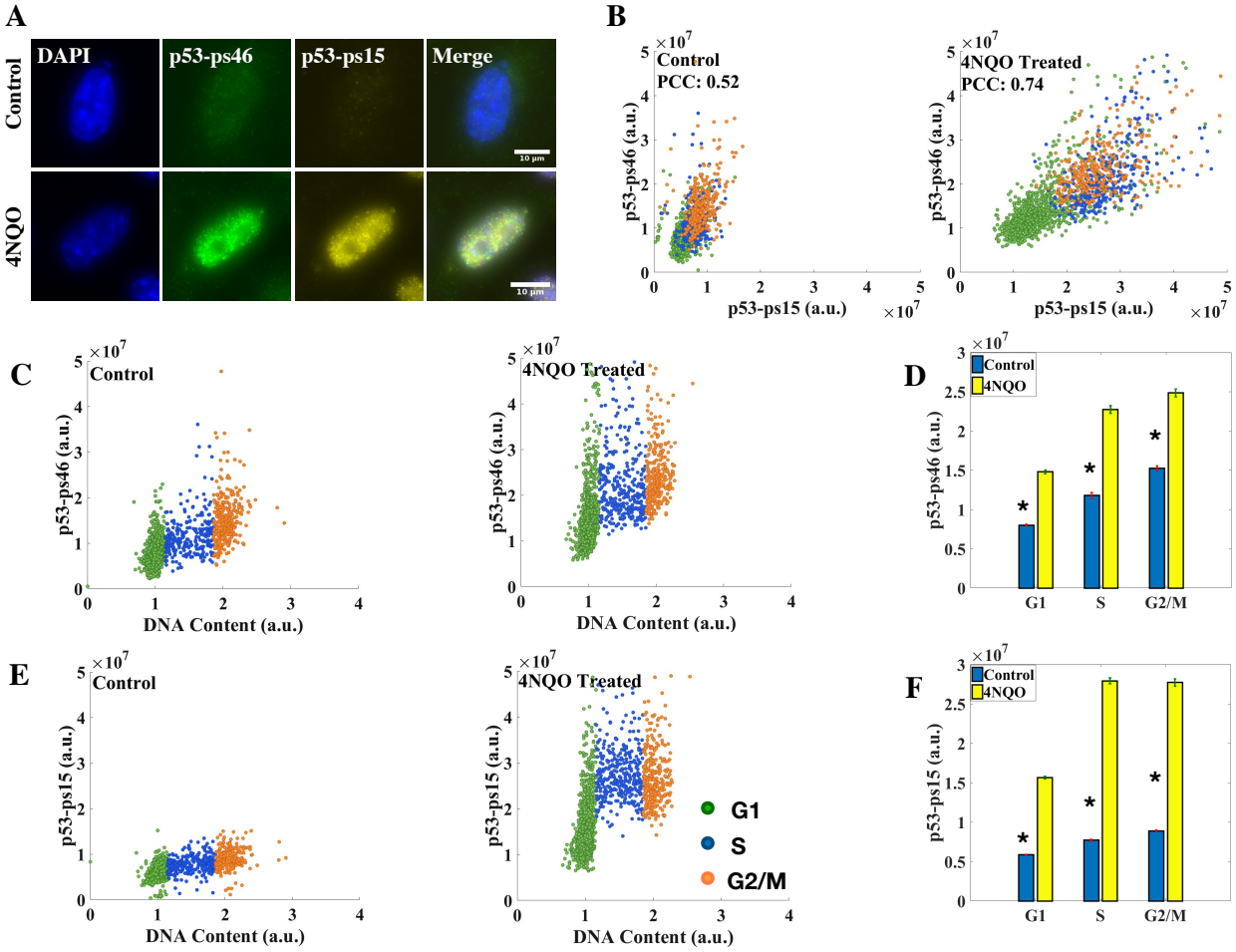

Supplementary Figure S4: Correlation between p53-ps46 and p53-ps15 increases in DNA damaged cells

(A) IF for p53-ps15 and p53-ps46 was performed on A549 cells (scale bar: 10 μm). (B) Correlation coefficient between p53-ps46 and p53-ps15 increased in DNA damaged (but non-apoptotic) cells. (C, E) Cell cycle distribution of p53-ps46 and p53-ps15. (D, F) Mean levels of p53-ps46 and p53-ps15 in respective cell cycle phases. All differences are significant with p-value < 0.05 (K-S test). (Errorbars are standard errors. The analysis was done on 1400 cells.)

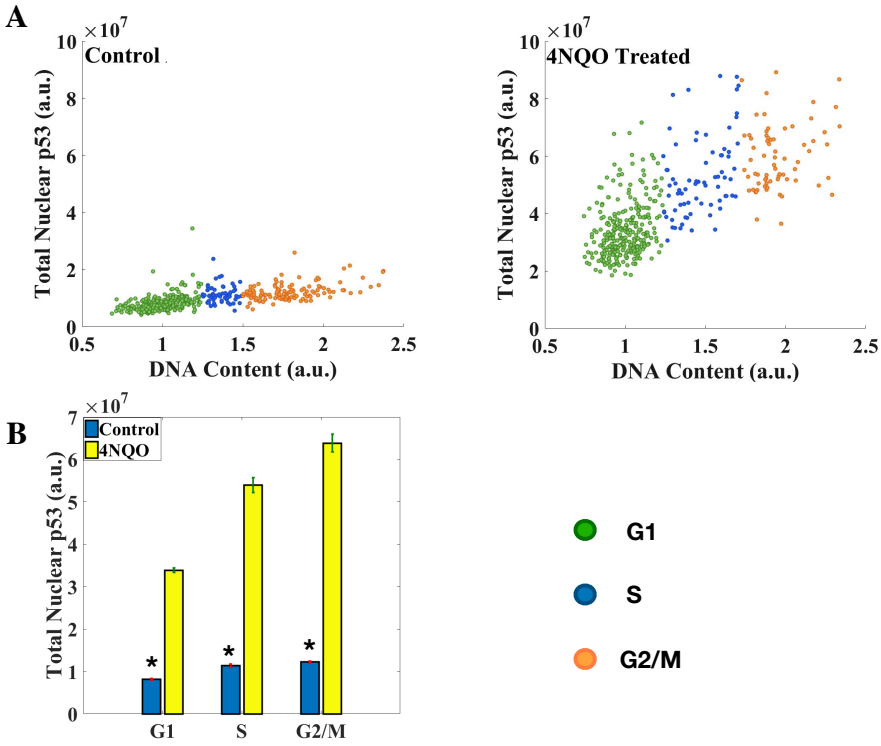

Supplementary Figure S5: Distribution of nuclear p53 with DNA content from IF combined with smFISH for *P53* in A549 cells

(A, B) Expression profile for nuclear p53 obtained from smFISH + IF matched with one obtained from just IF experiments. All the differences are significant with p-value < 0.05 (K-S test). Errorbars are standard errors. (The analysis was done on 444 cells.)

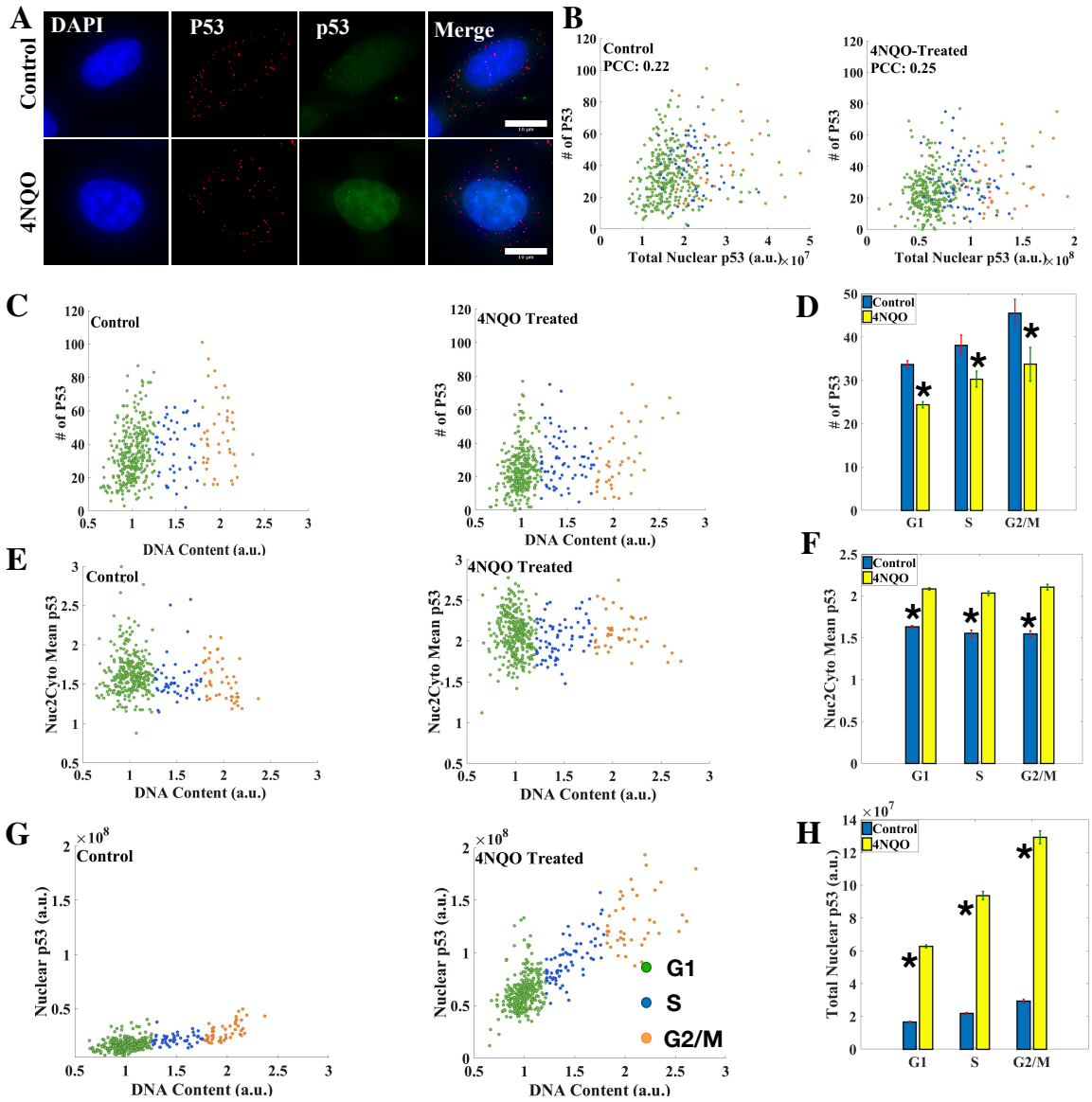

Supplementary figure S6-A: *P53* gene regulation in HeLa cells upon DNA damage
(A) smFISH was combined with IF for *P53* in HeLa cells (scale bar: 10 μm). (B) Correlation between *P53* mRNA number and protein levels remained poor in DNA damaged cells. (C) Cell cycle distribution of *P53* mRNA number. (D) Mean mRNA counts in DNA damaged and control cells in respective cell cycle phases. mRNA count was consistently and significantly lower in DNA damaged cells. The repression was at least 20% in all the phases of the cell cycle. (E) Cell cycle distribution of nuclear-to-cytoplasmic ratio of mean levels of p53. The average numbers of *P53* mRNA in control cells in G1-, S- and G2/M-phase of the cell cycle were 34 ± 1, 38 ± 2, 45 ± 3 while for DNA damaged cells they were 24 ± 1, 30 ± 2, 34 ± 4. (F) Nuclear to cytoplasmic ratio of mean levels of p53 protein went up in DNA damaged cells and remained constant throughout the cell cycle in both DNA damaged and control cells. (G) Cell cycle distribution of p53 protein levels in DNA damaged and control cells. Induction of p53 was observed in DNA damaged cells. Though p53 nuclear expression increased with the increase in DNA content, the nuclear-to-cytoplasmic ratio was maintained throughout the cell cycle. (H) Mean levels of nuclear p53 in different phases of the cell cycle followed the same trend as observed for A549 cells. All differences are significant with p-value < 0.05 (K-S test). (Errorbars are standard errors. The analysis was done on 311 cells.)

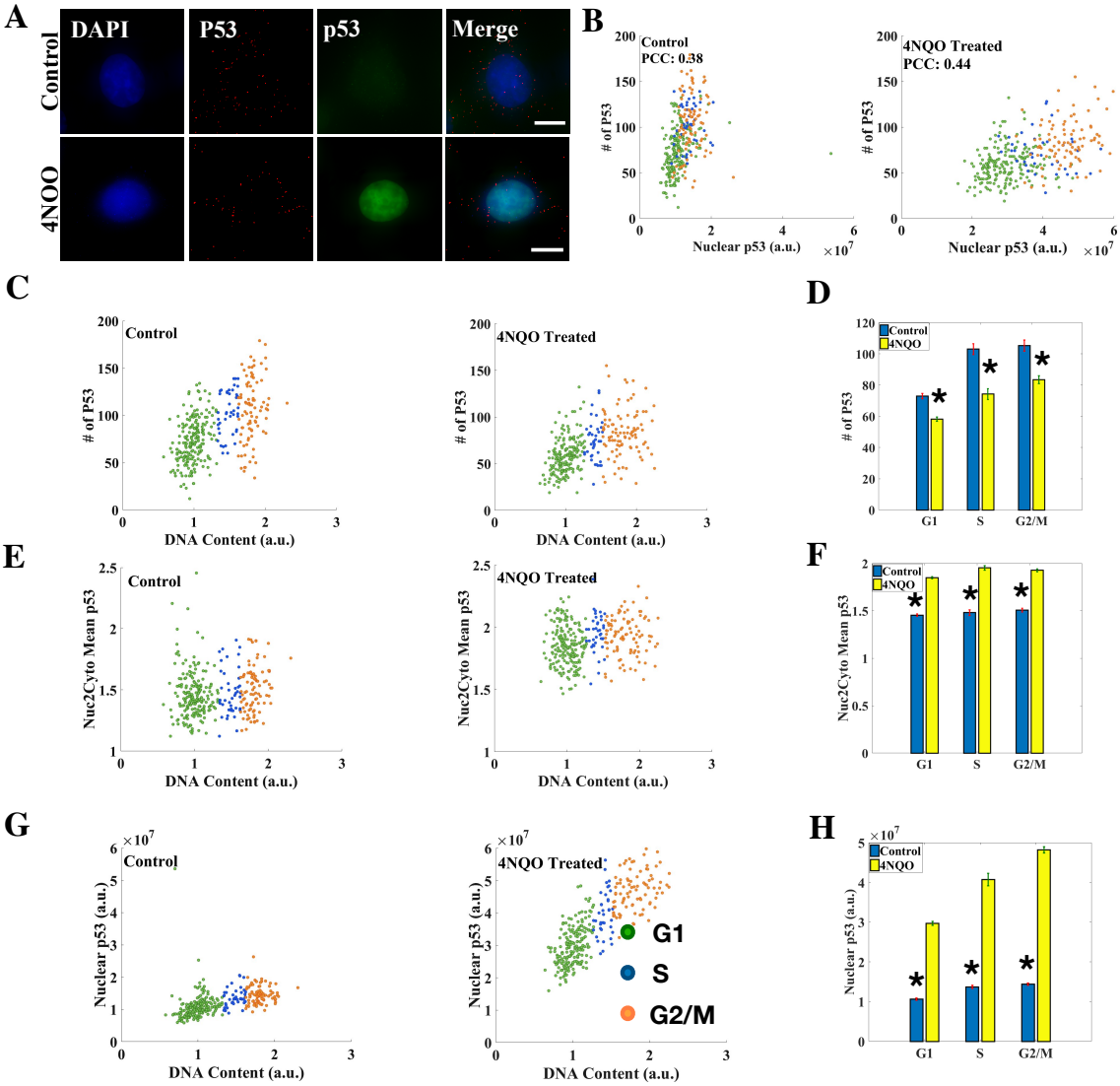

Supplementary figure S6-B: *P53* gene regulation in MCF7 cells upon DNA damage

(A) smFISH was combined with IF for *P53* in MCF7 cells (scale bar: 10 μm). (B) Correlation between *P53* mRNA number and protein levels remained poor in DNA damaged cells. (C) Cell cycle distribution of *P53* mRNA number. (D) Mean mRNA counts in DNA damaged and control cells in respective cell cycle phases. mRNA count was consistently and significantly lower in DNA damaged cells. The repression was at least 18% in all the phases of the cell cycle. (E) Cell cycle distribution of nuclear-to-cytoplasmic ratio of mean levels of p53. The average numbers of *P53* mRNA in control cells in G1-, S- and G2/M-phase of the cell cycle were 73 ± 2, 103 ± 4, 105 ± 4 while for DNA damaged cells they were 58 ± 1, 74 ± 3, 86± 3. (F) Nuclear to cytoplasmic ratio of mean levels of p53 protein went up in DNA damaged cells and remained constant throughout the cell cycle in both DNA damaged and control cells. (G) Cell cycle distribution of p53 protein levels in DNA damaged and control cells. Induction of p53 was observed in DNA damaged cells. Though p53 nuclear expression increased with the increase in DNA content, the nuclear-to-cytoplasmic ratio was maintained throughout the cell cycle. (H) Mean levels of nuclear p53 in different phases of the cell cycle followed the same trend as observed for A549 cells. All differences are significant with p-value < 0.05 (K-S test). (Errorbars are standard errors. The analysis was done on 250 cells.)

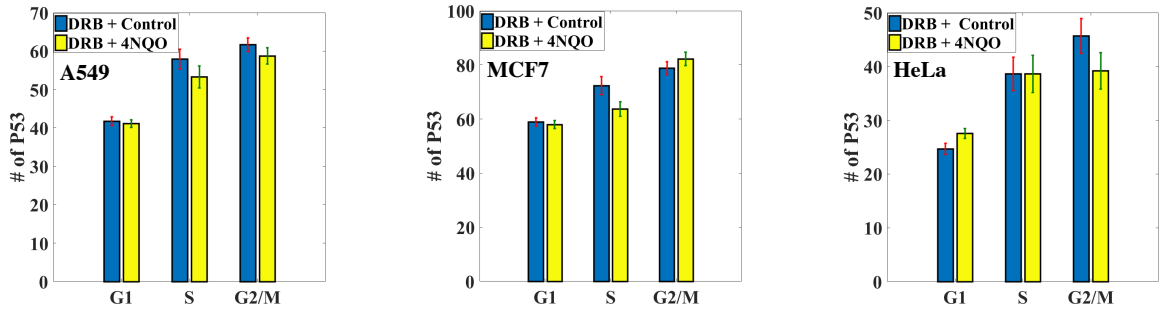

Supplementary figure S7: *P53* transcription is impaired during DNA damage
Transcription was blocked with DRB to investigate if the repression observed in *P53* transcript number was due to impaired transcription or increased degradation. We observed that in all the three cell lines—MCF7, A549 and HeLa—transcription block made the dip in transcript number decrease or disappear altogether. This suggests that P53 transcription is impaired during DNA damage. The analysis was done for at least 250 cells each.

Supplementary Table 1:

Probes Sequences (from 5' to 3')

CCNA2		CCNE1		Histone H4 (Hist1H4E)	
1	gtctgctgcaatgctagcag	1	aaaaacggtcacgtttgcct	1	cctttgccgcgaccagacat
2	ttttccgggttgatattctc	2	attttggccatttcttcatc	2	tcctttacccagtccctttc
3	aagatccttaaggggtgcaa	3	gcacagactgcattattgtc	3	ccttacggtgacgcttagcg
4	ggtgacatgctcatcattta	4	ttgtcaggtgtggggatcag	4	ccctggatgttatctcgcag
5	tgtttgctttccaaggagga	5	gtaaacccggtcatcatctt	5	ccggatggcaggcttggtaa
6	aatggtgaacgcaggctgtt	6	gaggcttgcacgttgagttt	6	acacccccgcgacgagcaag
7	tctttttctgcttcatccac	7	cctctggatggtgcaataat	7	gatgagaccagaaatgcgct
8	ttcagctggcttcttctgag	8	tatttgcccagctcagtaca	8	ttcagaaccccgcgagtctc
9	cttcacgctctatttttga	9	atgattttccagacttcctc	9	aatcacgttttccagaaaca

10	gctgaattaaaagccagggc
11	tctgggtccaggtaaactaa
12	aatcaagagggaccaatggt
13	tcaaaactaccatccattgg
14	catgtccatagtatgtggtg
15	cactggcttttcatcttcta
16	ggtagtctggtacttcatta
17	aggtatgtgtgaatatcctc
18	acatttaacctccatttccc
19	tcatgtaacccactttaggt
20	ttagtgatgtctggctgttt
21	cacgaggatagctctcatac
22	tctcctacttcaactaacca
23	gggtctcattctgtagttta
24	atcaatgtagttcacagcca
25	gcactgacatggaagacagg
26	acaagctgaagttttcctct
27	tgaggctaacagcatagcag
28	tgggggtatatttcttcaa
29	tgtacacaaactctgctact
30	ttggtgtaggtatcatctgt
31	agatgctccattctcagaac
32	gtcaaaagtaaggactttca
33	tgatttactgttggagcagc

10	agtatgtcttttccttgttt
11	gctcaagaaagtgctgatcc
12	atttttggctgcagaagagg
13	ccaatccagaagaattgctc
14	tatagacttcacacacctcc
15	gtaaaaggtctccctgtgaa
16	ggtcaaagaaatcttgtgcc
17	ttttcttgtgtcgccatata
18	atgaaatcccaataagctgt
19	agatttcctcaagtttggct
20	aactggtgcaactttggagg
21	aagctccatctgtcacatac
22	ggtgagaatttcatctcctg
23	cttaagggccttcataatca
24	tagtcaggggacttaaacgc
25	tatacattcagccaggacac
26	atttagatatgcaacctgca
27	gcagtagcacttcatgtaag
28	aagatttgctggggatactg
29	caacagctctgcaatctgta
30	attcaaggcagtcaacatcc
31	gcagcaagtataccataagg
32	cgagaaatgatacaaggccg
33	acctttgcatcaattcaga

10	ccgtgtaagtcacagcatca
11	actgtcttgcgtttggcgtg
12	gtagaccacatccatcgctg
13	tgcgtccctgtctcttcagc
14	tagccgccgaagccgtaaag

34	gctgctgatgcagaaagtat	34	ctatgtcgcaccactgatac	
35	ctttcaactttgcagtttgc	35	gaaccatccacttgacacag	
36	attctcccaaaaacattgct	36	tcccttataaccatggcaaa	
37	gggtcagcatctatcaaact	37	gaagtgcttcagttttgagc	
38	tgatggcaaatacttgaggt	38	tgtgcatcttcatcagcgac	
39	gaaaggcagctccagcaata	39	tgtctctgtgggtctgtatg	
40	gtgactgtgtagagtgctaa	40	gctttgtccagcaaatccaa	
41	aatgattcaggccagctttg	41	gacaacatggctttctttgc	
42	ggtatatccagtctttcgta	42	agaggagaagccctattttg	
43	gacaaggcttaagactttcc			
44	tttgaggtaggtctggtgaa			
45	tgactgttgtgcatgctgtg			
46	gaatttttgtacttttctct			
47	gttgaggagagaaacaccat			
48	acagatttagtgtctctggt			

Supplementary Table S1: The probes were designed in Stellaris Probe Designer by Biosearch Technologies and ordered from the same. The numbers of probes for CCNA2 and CCNE1 were 48 and 42 respectively. Because of the small gene size, *Histone H4* probes were limited to 14.